

# Pulmonary Delivery of Therapeutic and Diagnostic Gases

Warren M. Zapol, MD,<sup>1</sup> H. Cecil Charles, PhD,<sup>2</sup> Andrew R. Martin, PhD,<sup>3,\*</sup> Rui C. Sá, PhD,<sup>4</sup>  
Binglan Yu, PhD,<sup>1</sup> Fumito Ichinose, MD, PhD,<sup>1</sup> Neil MacIntyre, MD,<sup>5</sup> Joseph Mammarrappallil, MD, PhD,<sup>6</sup>  
Richard Moon, MD,<sup>7</sup> John Z. Chen, BSc,<sup>3</sup> Eric T. Geier, BSc,<sup>4</sup> Chantal Darquenne, PhD,<sup>4,\*</sup>  
G. Kim Prisk, PhD, DSc,<sup>4,8,\*</sup> and Ira Katz, PhD<sup>9,10,\*</sup>

## Abstract

The 21st Congress for the International Society for Aerosols in Medicine included, for the first time, a session on *Pulmonary Delivery of Therapeutic and Diagnostic Gases*. The rationale for such a session within ISAM is that the pulmonary delivery of gaseous drugs in many cases targets the same therapeutic areas as aerosol drug delivery, and is in many scientific and technical aspects similar to aerosol drug delivery. This article serves as a report on the recent ISAM congress session providing a synopsis of each of the presentations. The topics covered are the conception, testing, and development of the use of nitric oxide to treat pulmonary hypertension; the use of realistic adult nasal replicas to evaluate the performance of pulsed oxygen delivery devices; an overview of several diagnostic gas modalities; and the use of inhaled oxygen as a proton magnetic resonance imaging (MRI) contrast agent for imaging temporal changes in the distribution of specific ventilation during recovery from bronchoconstriction. Themes common to these diverse applications of inhaled gases in medicine are discussed, along with future perspectives on development of therapeutic and diagnostic gases.

**Keywords:** *in vitro* upper airway model, lung imaging, magnetic resonance imaging (MRI), nitric oxide, oxygen, pulmonary hypertension

## Introduction

THE 21ST CONGRESS for the International Society for Aerosols in Medicine included, for the first time, a session on *Pulmonary Delivery of Therapeutic and Diagnostic Gases*.<sup>(1)</sup> The rationale for such a session within ISAM is that the pulmonary delivery of gaseous drugs in many cases targets the same therapeutic areas as aerosol drug delivery, and is in many scientific and technical aspects similar to aerosol drug delivery. For example, the gaseous drug must be delivered by a medical device, through a patient interface, into the respiratory tract to a lung target, where it might be absorbed into the systemic circulation, all common aspects of

aerosol drug delivery. There are issues ranging from patient compliance for home use to delivery to ventilated patients in intensive care, which are also common to both medical gases and aerosols.

Consider more specific examples of inhaled medical gases: the most well-known inhaled gas with widespread and often critical therapeutic applications is oxygen. Oxygen therapy has, on occasion, been administered with unwarranted complacency; nonetheless, with the variety of settings (e.g., homecare versus hospital), patient interfaces (e.g., face masks and nasal cannulas), and sources (e.g., cylinders and concentrators) involved, it is difficult to assess optimal dosing and delivery modes.<sup>(2–7)</sup> The endogenous signaling molecule

<sup>1</sup>Anesthesia Center for Critical Care Research, Department of Anesthesia, Critical Care and Pain Medicine, Massachusetts General Hospital, Harvard Medical School, Boston, Massachusetts.

<sup>2</sup>Duke Image Analysis Laboratory, Center for Advanced MR Development, Department of Radiology, Duke University School of Medicine, Durham, North Carolina.

<sup>3</sup>Department of Mechanical Engineering, University of Alberta, Edmonton, Canada.

<sup>4</sup>Department of Medicine, University of California, San Diego, San Diego, California.

Departments of <sup>5</sup>Pulmonology, <sup>6</sup>Radiology, and <sup>7</sup>Anesthesiology, Duke University School of Medicine, Durham, North Carolina.

<sup>8</sup>Department of Radiology, University of California, San Diego, San Diego, California.

<sup>9</sup>Medical R&D, Air Liquide Santé International, Les Loges-en-Josas, France.

<sup>10</sup>Department of Mechanical Engineering, Lafayette College, Easton, Pennsylvania.

\*Member of ISAM.

nitric oxide (NO) is now widely used to treat pulmonary hypertension without systemic side effects.<sup>(8)</sup> However, there is growing evidence of beneficial systemic effects of NO that would make it protective after ischemic insult.<sup>(9,10)</sup> The therapeutic potential of other endogenous signaling molecules such as carbon monoxide<sup>(11,12)</sup> and hydrogen sulfide<sup>(13)</sup> are also being investigated.

The well-known anesthetic gas, nitrous oxide, shows potential as a treatment for chronic pain.<sup>(14,15)</sup> The noble gases have been shown to have interesting biological activity despite chemical inertness.<sup>(16)</sup> The most well-known application is xenon for anesthesia, providing relatively more stable intraoperative blood pressure, lower heart rate, and faster emergence from anesthesia than volatile and propofol anesthesia.<sup>(17)</sup> Helium has long been used as an aid to respiration due to its mechanical property of low density<sup>(18)</sup> and has potential to optimize aerosol deposition if used as a carrier gas.<sup>(19,20)</sup> Furthermore, diagnostic gases related to the imaging of ventilation are instrumental in understanding lung function, and thus the delivery of aerosols and the resulting deposition, as well as the benefits of aerosolized drugs in terms of improved ventilation.<sup>(21)</sup>

This article serves as a report on the recent ISAM congress session providing a synopsis of each of the presentations. Regarding therapeutic gas applications: Dr. Warren Zapol of Massachusetts General Hospital opened the session by describing the conception, testing, and development of the use of inhaled NO to treat acute and chronic pulmonary hypertension; and Dr. Andrew Martin of the University of Alberta showed how realistic adult nasal replicas, originally used for aerosol deposition studies, could be used to evaluate the performance of pulsed oxygen delivery devices. Presenting on diagnostic and imaging gases were Dr. Cecil Charles of Duke University, who gave an overview of several diagnostic gas modalities; and Dr. Rui Carlos Sá from the University of California, San Diego, who concluded the session with a presentation on the use of inhaled oxygen as a proton magnetic resonance imaging (MRI) contrast agent for imaging temporal changes in the distribution of specific ventilation (SV) during recovery from bronchoconstriction.

### NO for the Treatment of Pulmonary Hypertension

A therapeutic potential for inhaled NO to act as a selective pulmonary vasodilator was first demonstrated by Frostell et al. in 1991, who showed that breathing NO gas produced rapid and profound pulmonary vasodilation in an awake lamb model of pulmonary hypertension produced by infusion of the stable thromboxane analog U46619, a potent pulmonary vasoconstrictor.<sup>(22)</sup> NO rapidly reacts with oxyhemoglobin to form methemoglobin and nitrate, and with deoxyhemoglobin to form iron nitrosyl hemoglobin.<sup>(23,24)</sup> Therefore, the vasodilatory effect of inhaled NO is effectively limited to the lung. This is in sharp contrast to intravenously infused vasodilators that also produce systemic vasodilation and can lead to systemic arterial hypotension.<sup>(25)</sup> This unique ability of inhaled NO to cause highly selective pulmonary vasodilation has prompted a large number of preclinical and clinical studies.<sup>(26-29)</sup>

The early pilot studies demonstrated that inhaled NO therapy rapidly improves oxygenation without causing systemic hypotension in critically ill newborns with acute

pulmonary hypertension.<sup>(28,30)</sup> Subsequently, the efforts of many research groups studying newborns led to approval of inhaled NO by the U.S. Food and Drug Administration in 1999.<sup>(31)</sup> Since approval, inhaled NO has been commonly used to perform diagnostic procedures and treat a spectrum of cardiopulmonary conditions, including pulmonary hypertension.<sup>(32,33)</sup> Inhaled NO has saved the lives of hundreds of thousands of babies with persistent pulmonary hypertension and adults with pulmonary arterial hypertension before and after cardiac surgery.

Recent studies suggest that inhaled NO may prevent ischemia-reperfusion injury and reduce hemolysis-induced vasoconstriction and renal failure after cardiopulmonary bypass.<sup>(34)</sup> However, wider use of NO therapy is limited, because the current NO delivery systems using high pressure cylinders are cumbersome and expensive.<sup>(35)</sup> Inhaled NO therapy based on cylinder gas is only available in hospitals for inpatient use in some developed countries, but unavailable in many parts of the world, and not available anywhere for outpatient use. Several methods have been used to produce NO for biomedical purposes.<sup>(36-40)</sup> However, these methods produce large amounts of nitrogen dioxide (NO<sub>2</sub>) and ozone (O<sub>3</sub>) as toxic byproducts, requiring complex purification systems.<sup>(41,42)</sup> We have designed, developed, and tested a simple, portable, and economic NO generation device, producing NO by pulsed electrical discharge in air for inhalation therapy (Fig. 1).<sup>(43)</sup>

We have first tested whether our novel design NO generator produces therapeutic ranges (5–80 parts per million [ppm]) of NO from ambient air or an O<sub>2</sub>-enriched mixture at the bedside. We showed that NO production at atmospheric pressure varies with changing O<sub>2</sub> and N<sub>2</sub> levels, with maximal NO produced at 50% O<sub>2</sub>.<sup>(43)</sup> Then, we optimized our NO-generating device to yield maximal NO levels with minimal NO<sub>2</sub> and O<sub>3</sub> production. Our results demonstrated that iridium electrodes produce NO with minimal amounts of NO<sub>2</sub> in comparison to other electrode metals, such as stainless steel, nickel, and tungsten. To reduce NO<sub>2</sub> levels in the electrically generated NO, we use Ca(OH)<sub>2</sub>, a common CO<sub>2</sub> scavenger widely used in clinical ventilators. We demonstrated that 12 g of Ca(OH)<sub>2</sub> sufficiently reduces O<sub>3</sub> and NO<sub>2</sub>

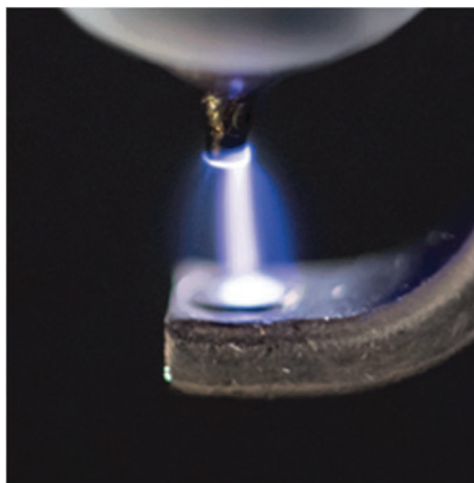


**FIG. 1.** Producing NO by pulsed electrical discharge.<sup>(43)</sup> NO, nitric oxide.

to levels well below Environmental Protection Agency (EPA) standards, without impairing NO production.

In anesthetized and mechanically ventilated lambs (body weight  $\sim 30$  kg), we have investigated whether plasma-generated NO could reduce pulmonary hypertension acutely induced by an infusion of U46619.<sup>(43)</sup> We concluded that electrically generated NO is as effective as NO delivered from a conventional cylinder. That is, at the same inhaled NO doses, electrically generated NO and NO diluted from a cylinder equivalently reduce pulmonary arterial pressure and pulmonary vascular resistance in lambs with pulmonary hypertension.

Because electrodes undergo erosion after prolonged electric NO generation,<sup>(44,45)</sup> we sought to optimize the purity and safety of NO generated by our device. Applying scanning electron microscopy and energy-dispersive X-ray spectroscopy, we detected and determined the metal particles (iridium, platinum, and nickel) released from the electrodes after plasma NO generation.<sup>(46)</sup> We then tested whether a  $0.22\ \mu\text{m}$  high-efficiency particulate air (HEPA) filter, placed in series with the NO generator, could capture all the metal particles in the effluent gas stream. Our data suggest that one single HEPA filter can effectively remove all metal particles released from the electrodes when generating electric plasma NO.<sup>(46)</sup>

To examine the safety of breathing electrically generated NO for a prolonged period of time, we have investigated whether it produces lung inflammation and/or metal deposition in mice lungs after breathing 50 ppm electrically generated NO in air for 28 days. We found that all the murine airway tissues, including tracheobronchial tissue and tissue of the distal lung, from both control (breathing air only) and mice breathing 50 ppm electric NO were normal and free of metal particles.<sup>(46)</sup> Taken together, these results indicate that prolonged inhalation of electrically generated NO is safe.

In a proof-of-concept human study, we examined the effects of breathing electrically generated NO in six healthy volunteers and six patients with chronic pulmonary hypertension.<sup>(47)</sup> Our data suggest that the synthesis and testing of electrically generated NO in a hospital setting were safe. No adverse effects were observed in the six healthy volunteers breathing 25 ppm NO in air for 10 minutes. In the six patients with chronic pulmonary hypertension, electric generation of NO led to acute pulmonary hemodynamic effects (e.g., reduced pulmonary vascular resistance) and the vasodilatory effect was equivalent to that of NO obtained from commercially available cylinders.

Inhaled NO is the first vasodilator to produce truly selective pulmonary vasodilation. A large number of laboratory and clinical research studies have been performed to delineate the biochemistry, physiology, side effects, and clinical efficacy of breathing NO in various diseases of children and adults. For many, it is lifesaving. The recent development of the electric generation of NO from air offers the potential for delivering NO gas for inhalation for prolonged periods in ambulatory or outpatient care settings. The device could also expand the delivery of NO to hospitals and clinics around the world because electric plasma NO generation is economical, easy to use, and safe. In future studies, we will focus on improving power supply efficiency, to increase NO production with less energy

consumption, and miniaturizing the size and weight of the portable device to less than one pound. If possible in the future, the size of our NO generation device will be phone sized and powered by portable batteries.

### Evaluation of Pulsed Oxygen Delivery in Realistic Adult Nasal Replicas

Long-term oxygen therapy (LTOT) is widely used in the treatment of chronic respiratory diseases. For patients with hypoxemic chronic obstructive pulmonary disease (COPD), LTOT administered for 15 hours/d or more has been demonstrated to improve survival time.<sup>(48)</sup> In the United States, over 1 million patients receive LTOT,<sup>(49)</sup> with Medicare reimbursements for oxygen-related costs exceeding 2 billion U.S. dollars in 2011 for COPD patients.<sup>(50)</sup> Despite the wide use of oxygen in the treatment of respiratory diseases, firm evidence of LTOT's benefits is lacking in mild-to-moderate disease.<sup>(49,51)</sup> The work described below was motivated, in part, by the belief that more conclusive demonstration of the benefit (or lack of benefit) of LTOT may follow better understanding of, and consistency in, oxygen delivery and dosing. Oxygen administration is generally prescribed and discussed as continuous flow of oxygen (CFO), with dosing quantified in liters per minute (L/min) of oxygen delivered to a patient interface at a steady flow rate.

However, to enable mobility of patients receiving LTOT, portable sources of oxygen are frequently employed, including small gas cylinders, portable liquid dewars, and portable oxygen concentrators (POCs). These portable sources typically do not supply oxygen at continuous, steady flow rates. Rather, to extend usage of portable sources with limited capacity, an oxygen conserving equipment is used to administer oxygen in short pulses, or boli, triggered to coincide with patient inspiration. In this manner, oxygen is delivered early in the breath, so that the fraction of oxygen exhaled from the anatomical dead space is reduced, and efficiency of administration is improved compared with CFO.

Ideally, the volume of oxygen delivered per breath in pulses from portable sources would be similar to that for CFO at a specified flow rate, so that pulse settings on portable sources (e.g., pulse setting of 1, 2, or 3) could be interpreted in terms of nominally equivalent CFO flow rates (e.g., of 1, 2, or 3 L/min). This is not currently the case. The most recent update to the ISO standard *Particular requirements for basic safety and essential performance of oxygen conserving equipment*<sup>(50)</sup> notes that because numerical dose settings on oxygen conserving equipment might not correlate to CFO flow rates, these settings may be misinterpreted and result in incorrect oxygen delivery. The potential for confusion is exacerbated as different portable oxygen sources (e.g., POCs from two different manufacturers) may deliver different volumes of oxygen at nominally equivalent pulse settings. As a result, the use of a conserving equipment employing pulsed oxygen delivery requires patient titration to ensure proper settings are selected on a particular source device, to provide adequate arterial oxygen saturation ( $\text{SaO}_2$ ).<sup>(50)</sup>

To investigate equivalency between pulsed and continuous oxygen delivery through nasal cannula, Chen et al.<sup>(52)</sup>

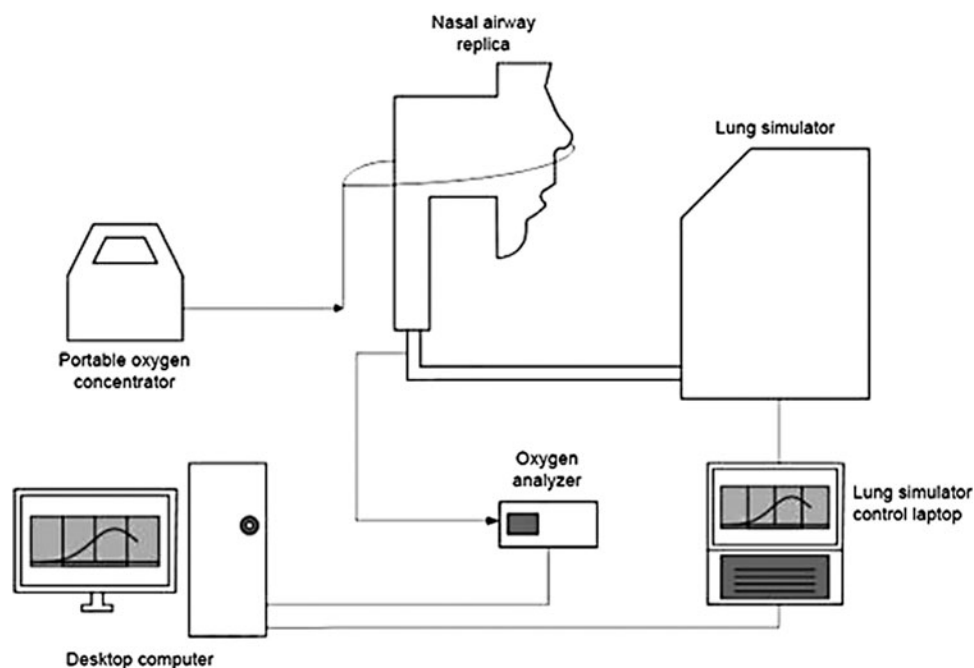


**FIG. 2.** Experimental apparatus used to evaluate oxygen delivery using realistic nasal airway replicas. Arrows indicate direction of gas flow. Adapted from Chen et al.<sup>(52)</sup>

have recently developed *in vitro* methods using realistic nasal airway replicas (Fig. 2). Oxygen delivery through nasal cannula was tested for pulsed delivery from a POC and compared with CFO delivered from a stationary compressed oxygen cylinder. A test lung simulated three breathing patterns representative of a COPD patient at rest, during exercise, and while asleep. Volume-averaged fraction of inhaled oxygen ( $F_iO_2$ ) was calculated by analyzing the oxygen concentration in gas sampled at the exit of each replica (representing “tracheal” concentrations) and inhalation flow rates over time.  $F_iO_2$  could then be compared between numerical pulse settings and nominally equivalent CFO flow rates.

While the use of realistic, and idealized, upper airway replicas has been frequent in research related to pharmaceutical aerosol administration [e.g., Byron et al.<sup>(53)</sup>, Grgic et al.<sup>(54)</sup>, and Golshahi et al.<sup>(55)</sup>], previously, only highly simplified geometries have been used for evaluating delivery of medical gases.<sup>(56,57)</sup> For pulsed gas delivery, the use of realistic airway replicas allows *in vitro* testing to be conducted under more realistic triggering conditions. Chen et al. observed instances of failure to trigger pulse delivery for four of the fifteen airway replicas they employed.<sup>(52)</sup> Where pulse delivery was triggered during inspiration,  $F_iO_2$  was consistently lower for pulsed delivery than for CFO. Differences between pulsed delivery and CFO were largest when higher numerical pulse setting was combined with breathing parameters typical of sleeping patients.

This was likely attributable to two factors: for CFO, the effect of oxygen pooling in the nasal cavity near the end of expiration boosts  $F_iO_2$  for slower and shallower breathing, whereas for pulsed delivery, lower inspiratory flow rates result in delayed triggering and hence delayed arrival of the oxygen pulse, leading, in some cases, to retention of de-

livered oxygen in the upper airways and subsequent exhalation of part of the delivered oxygen pulse.

Although the results presented by Chen et al. are specific to the single commercial POC tested, additional testing using their methodology may provide valuable information describing relative oxygen delivery from different devices operating at nominally equivalent numerical settings.

### Diagnostic Gases: Imaging and Lung Function Testing

Evaluation of the delivery of inhaled therapeutics faces special challenges compared to oral or injected agents. The nature of the agent (dry particles vs. aerosols) and the nature of the delivery device (e.g., metered dose and nebulizer) can have an impact on the delivery of the agent.<sup>(58)</sup> While direct evaluation of the delivery can be addressed with imaging techniques, there are a number of limitations to the current techniques. Imaging the deposition of an inhaled agent is challenging and generally limited to radioisotope imaging (e.g., planar nuclear scintigraphy, Single Photon Emission Computed Tomography [SPECT], and Positron Emission Tomography [PET]).

The advantages and disadvantages have been reviewed previously,<sup>(58)</sup> but include costs, limited spatiotemporal resolution, the need to synthesize labeled drug (PET), or physically combine a radiotracer with the agent (SPECT, Scintigraphy). From an imaging perspective, evaluation of nuclear medicine strategies can be used to evaluate pharmacokinetics, that is, distribution. Other regional strategies such as hyperpolarized gas Magnetic Resonance Imaging (hpMRI) and fluorine-19 Magnetic Resonance Imaging (<sup>19</sup>F MRI) could be used to evaluate response to treatment or pharmacodynamics. Since mammalian lungs function by a convection/diffusion mechanism and multiple breaths are

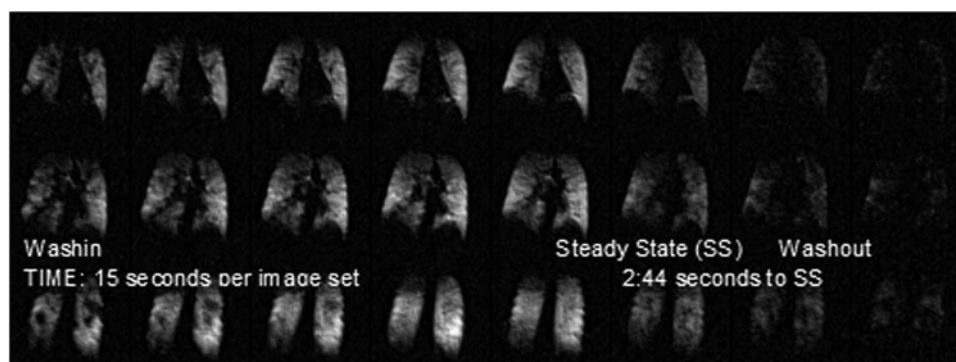


**FIG. 3.** Functional lung images from a subject with COPD. Each of the frames shows one slice from a 3D image obtained during a single deep breath-hold. The images are obtained using an approach of three tidal breaths followed by the single deep breath-hold and this is repeated several times until a steady state is obtained. The time frame from image to image is generally 30–45 seconds depending on the subject's respiration rate. Much like hyperpolarized gas Magnetic Resonance Imaging (hpMRI), the early frames show areas that have been described in the hpMRI literature as “ventilation defects” or areas of no or poor ventilation. As is evident in the time axis (left to right), these actually describe “slow filling” compartments of the lung. Since the gaseous agent does not reach these areas in a single breath, it is likely the distribution of inhaled agent would be similar. 3D, three dimensional; COPD, chronic obstructive pulmonary disease.

required to fully exchange the gases in the lung, it would be useful to understand and measure the regional lung function as a factor in inhaled drug delivery. Poor ventilation could certainly have a negative impact of drug delivery and response to treatment, especially when relying on single breath delivery. This has been demonstrated in several reports where nonuniform distribution of radiotracers in subjects with lung disease is contrasted to more uniform distribution in subjects with normal lung function.<sup>(59–65)</sup>

There have also been several approaches proposed for modeling delivery of inhaled agents, as described in the article by Darquenne et al.<sup>(21)</sup> An alternative strategy to address these problems is to start with an actual evaluation of lung ventilation patterns in the absence of the agent using an imagable gas. Clearly, if there are poorly ventilated regions of the lung [i.e., slow filling compartments<sup>(66)</sup>], then any single breath delivery system could be impacted negatively, in that, the regions of the lung that may be most in need of the treatment are less likely to receive the treatment agent.

For example, Figure 3 shows ventilation images of three slices extracted from a three-dimensional (3D) volume image of the lung from a subject with COPD. These images were obtained using an <sup>19</sup>F MRI and taken over a series of breaths of a gas mixture (79% perfluoropropane and 21% oxygen) followed (after steady state) by washout, while breathing room air.<sup>(67)</sup> Each 3D set was taken in a 15-second breath-hold with three tidal breaths preceding each image acquisition. It is clear that a significant fraction of the lung exhibits slow filling compartments, and in the first frame, it is apparent that there are areas of the lung that are not ventilated at all.

Figure 4 shows a parametric image from two slices, where the image intensity scale represents the ventilation time constant in seconds for each of the regions of the lung. In this subject, 43.7% of the lung volume has wash-in time constants  $\geq 60$  seconds and ranging up to  $\sim 600$  seconds.

With long time constants (in excess of 60 seconds), it is understandable that an inhaled agent may have poor activity in those regions.

Moving from a pharmacokinetic evaluation of drug delivery to a pharmacodynamic evaluation of change in lung ventilatory function postinhalation opens a new window for evaluation of inhaled drugs with excellent spatial and temporal resolution. In the spatial sense, <sup>19</sup>F MRI can evaluate lung function at the level of a few acini. In the temporal sense, <sup>19</sup>F MRI can measure changes from tens of seconds to minutes, to hours to days. The lack of ionizing radiation and the inert nature of the imaging visualization agents allow repeated measurements over a range of time frames that should address the needs of any new (or old for that matter) inhaled aerosolized agent.

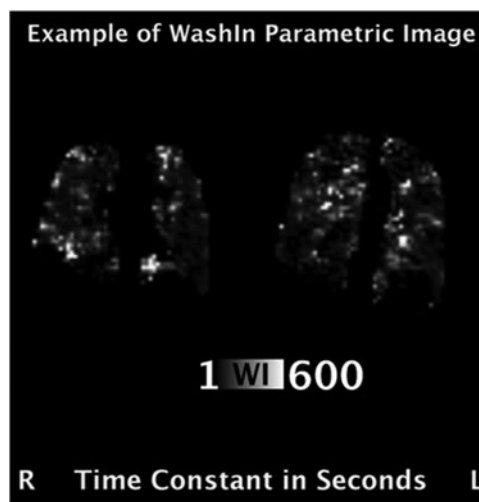


**FIG. 4.** Parametric images calculated pixelwise from the time series data show the distribution of “slow filling” compartments of the lung, and the fraction of lung volume that has such poor ventilation can easily be determined.

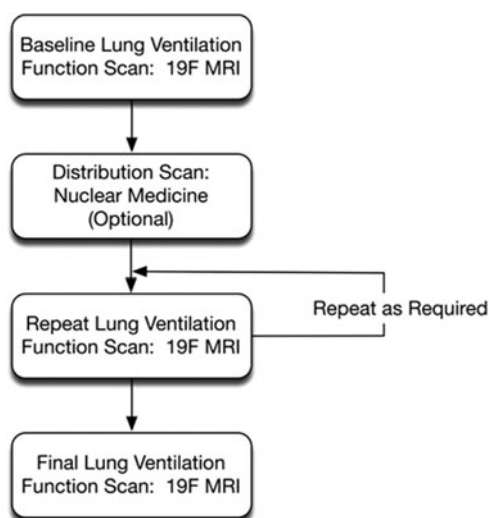


**FIG. 5.** A possible evaluation strategy for pharmacokinetic/pharmacodynamic evaluation of inhaled therapeutic agents.

One can consider a treatment schema such as shown in Figure 5, where after a baseline ventilatory evaluation, multiple posttreatment evaluations are possible over a variety of time frames, for example, minutes for short-acting agents such as rescue inhalers to hours or days for long-acting agents. Thus, new agents can be tested in the target population using the planned delivery device. In addition, a nuclear medicine scan (PET, SPECT, and Scintigraphy) of distribution of the agent could be added after the baseline ventilation function scan for distribution analysis. Clearly, early evaluation of agents in this manner could impact changes in the formulation or the actual delivery unit, with direct evidence of activity of the agent.

### Imaging Temporal SV Using Oxygen as an MRI Contrast Agent

Oxygen, in addition to its therapeutic use, has historically been used as an inhaled “contrast” agent to probe ventilation heterogeneity in the lung, namely for measuring SV, the ratio of fresh gas entering a lung region to its regional end tidal volume. The multiple breath washout is a classical pulmonary function test,<sup>(68)</sup> which allows for the quantification of heterogeneity of specific ventilation (SV). Typically, the multiple breath washout follows the nitrogen washout concentration on a breath-by-breath basis, following a sudden change in inspired oxygen concentration, typically from room air to 100% O<sub>2</sub>.

Different indices have been used throughout the years, with the Lung Clearance Index (LCI) being the simplest and more commonly used.<sup>(69)</sup> More complex metrics such as Sacin and Scnd<sup>(70)</sup> and the width of the SV distribution<sup>(71)</sup> are also common. Multiple-breath washout uses a fast responding gas analyzer (often a mass spectrometer) to measure the nitrogen concentration at the mouth, and thus does not provide spatial information.

SV imaging is an MRI technique that is similar to multiple-breath washout tests, with the major difference that the measurement of gas concentration is not performed at the mouth as in multiple-breath washout, but spatially

throughout the lung, using an MRI scanner. It was made possible by the finding that oxygen dissolved in tissues shortens the T1 relaxation time and can thus be used as a contrast agent.<sup>(72)</sup> Thus, appropriately prepared and timed MR images can sense local changes in oxygen concentration, following sudden changes in inspired oxygen fraction (F<sub>I</sub>O<sub>2</sub>)—wash in and washout of inhaled oxygen.

The first application of oxygen-enhanced MRI was to identify nonventilating regions of the lung.<sup>(72,73)</sup> Our work has extended this ventilated/unventilated binary approach to create quantitative regional SV information.<sup>(74)</sup> As in multiple-breath washout tests, regional (alveolar) partial pressure of oxygen (P<sub>A</sub>O<sub>2</sub>) is determined by F<sub>I</sub>O<sub>2</sub> and other factors, such as local V/Q ratio; however, the rate of change of regional P<sub>A</sub>O<sub>2</sub> is dominated by the regional SV.<sup>(75)</sup> Quantification of SV is achieved by comparing the rate of change in the MRI signal following consecutive sudden changes in F<sub>I</sub>O<sub>2</sub>, with a library of modeled ideal lung units with different imposed SVs<sup>(76)</sup> responding to the same stimulus.

In a validation study against multiple-breath washout,<sup>(76)</sup> SV imaging was shown to produce comparable estimates of heterogeneity, and have acceptable test-retest repeatability. Previous applications of this technique have focused on the gravitational gradient of SV,<sup>(74)</sup> the distribution of SV during exercise,<sup>(77)</sup> and ventilation heterogeneity in subjects susceptible to High-Altitude Pulmonary Edema (HAPE).<sup>(78)</sup>

As developed and typically applied, SV imaging produces a quantitative map acquired over a ~20-minute period, representing the average ventilation pattern over the acquisition time. We extended our previous work by adding a temporal axis of recovery from an intervention, namely a methacholine challenge, allowing for a quantitative pharmacodynamic evaluation of the response to an induced asthma challenge.

To capture the regional temporal dynamics of recovery from methacholine-induced bronchoconstriction (predetermined PC<sub>20</sub> dose), we developed a sliding window analysis with a temporal resolution of ~7 minutes. Ventilation maps were acquired over ~18 minutes, starting <10 minutes after methacholine administration, in two healthy controls and two mild asthmatics (26±7, 22±2 years-old, FEV1 100±9, 101±1% predicted, PC<sub>20</sub> 10±8, 0.8±0.4 mg/mL of methacholine, for control and asthmatic patients, respectively). Respiratory-gated images were acquired using a 1.5T MRI scanner in the supine posture at functional residual capacity in 15-mm-thick sagittal slices (right lung)—with an in-plane resolution of 1.6×1.6 mm—using an inversion recovery fast spin echo sequence (inversion time 1.1 seconds), while subjects breathed alternating blocks of air and 100% O<sub>2</sub>. Up to four contiguous right lung slices were acquired, covering ~70% of the right lung.

Methacholine resulted in preferential constriction in the dependent lung (Fig. 6): averaged over all subjects, the fraction of constricted voxels, defined as the percentage of voxels where SV decrease by >50% from baseline to postconstriction was 57%±20% in the dependent lung and 38%±25% in the nondependent lung. This preferential dependent lung impact of inhaled methacholine is more expressive in the two healthy subjects studied (51%±10% and 19%±1%, dependent and nondependent, respectively) than in the two asthmatics (62%±30% and 56%±24%, dependent and non-dependent, respectively) (Fig. 6, right panel).

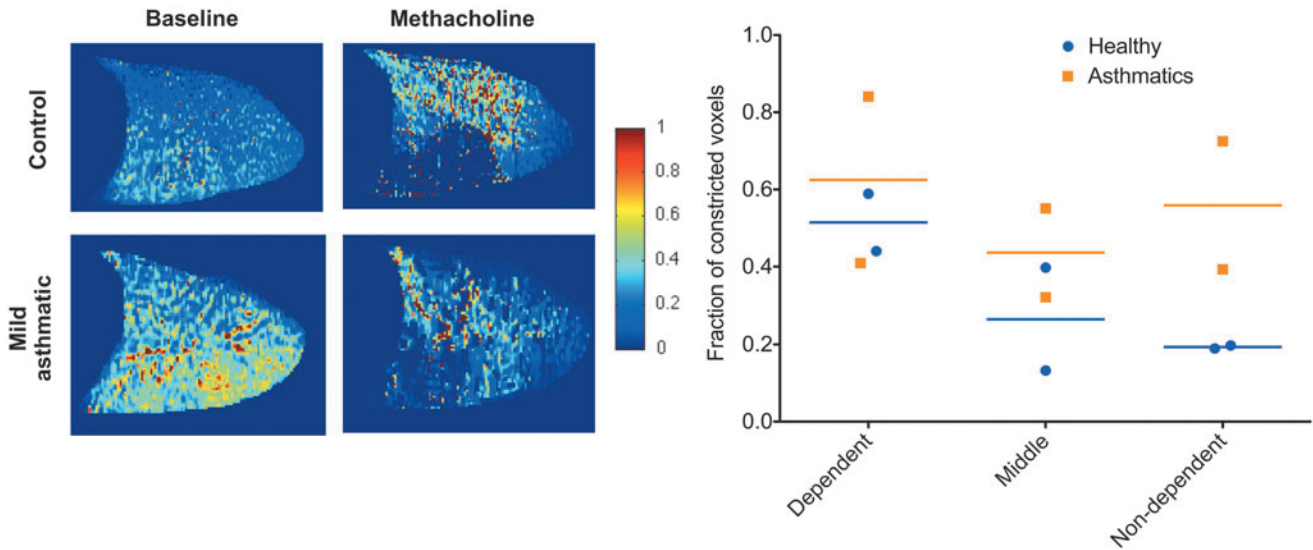


**FIG. 6.** Left panel: specific ventilation maps in a sagittal slice of the right lung in a healthy control (top row) and a mild asthmatic (bottom row) at baseline, and following methacholine-induced bronchoconstriction. In these sagittal images, the head is to the right, and the dorsal lung is toward the bottom of the images. Administration of the predetermined methacholine PC20 dose altered the pattern of specific ventilation, mostly in the dependent lung. Right panel: fraction of constricted lung in the dependent, middle, and nondependent lung thirds, constriction defined as a decrease in specific ventilation of  $\geq 50\%$ , for the two healthy (circles, blue lines) and two asthmatics studied (square, orange line).

The postprocessing temporal dynamics approach is illustrated in Figure 7, for a mild asthmatic subject. SV imaging data acquired after methacholine inhalation over 18 minutes was partitioned into three consecutive 7-minute windows (25% overlap), resulting in three consecutive spatial maps, showing the spatial pattern of recovery from the challenge. Overall, data showed a tendency for faster recovery from bronchoconstriction in asthmatics than in healthy controls, potentially driven by the lower methacholine doses and/or the repeated exposure to exacerbations and bronchoconstriction.

These preliminary data suggest that SV imaging can be used to quantify the regional temporal behavior of the lung following bronchoconstriction. Our technique, as with  $^{19}\text{F}$  MRI presented above, allows for the definition of biomarkers for the quantification of the regional impact of inhaled drugs or other respiratory interventions (deep inspirations and systemic drugs) with spatial resolution of the order of a few acini, and temporal resolution of  $\sim 5$  to 7 minutes. Oxygen-enhanced ventilation imaging shares most of the advantages of  $^{19}\text{F}$  MRI—good spatial resolution, no ionizing radiation,

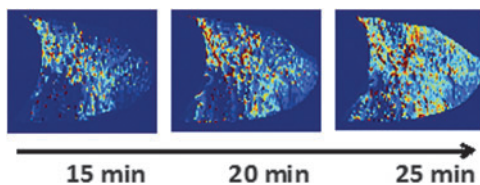


**FIG. 7.** Specific ventilation maps of a 15 mm sagittal slice of the right lung (same as in Fig. 6, mild asthmatic, bottom row), showing the time course of recovery following methacholine-induced bronchoconstriction (1 mg/mL) in a mild asthmatic. A 7-minute overlapping sliding window approach, centered at 15, 20, and 25 minutes after methacholine was applied, opening a window into the dynamics of the recovery from an induced asthma challenge.

and ability to perform repeated measures. It does have a more limited temporal resolution (minutes)—the poorer signal-to-noise ratio of oxygen-enhanced MRI, when compared to  $^{19}\text{F}$  MRI, requires longer acquisition time—yet it is easier to envision its general use, as it only requires readily available oxygen and standard, widely available proton MRI.

Another potential application of MR functional ventilation imaging is in the development and optimization of inhaled aerosolized drugs. In a recently published study, we combined SV Imaging with gamma scintigraphy to compare the regional distribution of ventilation with the deposition of  $5\ \mu\text{m}$   $^{99\text{m}}\text{Tc}$ -labeled inhaled particles. In healthy subjects, we showed that peripheral deposition and ventilation are proportional.<sup>(79)</sup> Combining quantitative MR ventilation imaging with particle deposition measurements has the potential to enable the early evaluation of inhalable drugs and contribute to optimization of their targeted delivery through manipulation of actionable characteristics such as resident gas properties, time/depth of inhalation, and particle size.

## Discussion and Conclusion

The congress session reported on in this article has illustrated some of the opportunities as well as the scientific and technical challenges regarding the *Pulmonary Delivery of Therapeutic and Diagnostic Gases*. Considering therapeutic gases, inhaled NO stands out as a proven and highly effective treatment of persistent pulmonary hypertension of the newborn and pulmonary hypertension following cardiac surgery. Outside of these indications, the use of NO, for example, in acute lung injury or acute respiratory distress syndrome, remains controversial, but as presented by Zapol, the potential to expand use of NO to new indications may be buoyed by the development of less expensive supply and sophisticated delivery devices.

It can be noted that therapeutic medical gas dosing runs the gamut from <100 up to one million ppm (i.e., 100%). Even greater concentrations, or gas partial pressures, may be obtained if hyperbaric applications are considered. Thus, accurate dosing (as illustrated by Martin for oxygen) requires expert knowledge in a complex marriage between medical device technology and physiology, expertise that has been applied to aerosol medicine and exhibited within ISAM for several decades. Similar to methods used in medical aerosol research, realistic or simplified upper airway geometries have been employed to evaluate the influence of gas delivery parameters on inhaled gas concentrations.<sup>(56,57)</sup> Analytical models have also been developed to estimate medical gas transport and uptake in the lungs.<sup>(80,81)</sup> Such tools could be valuable in the design of therapeutic gas delivery systems, and in evaluating contrasting modes of delivery.

On the other hand, the presentations by Charles and Sá show that diagnostic gases have much to offer the aerosol community and could be better integrated into clinical care. However, clearly, the obvious advantage of the type of forum provided by the ISAM congress is the direct exchange of information and exposure to conceptual new applications. For example, the MRI imaging technique, described by Sá to quantify SV, could be adapted to measure the effectiveness of oxygen delivery as explained by Martin. In conclusion, perhaps ISAM could provide a forum for medical gases similar to the role it has played for medical aerosols.

#### Author Disclosure Statement

W.M.Z. and B.Y. are inventors on patents filed by MGH on the electric generation of NO. W.M.Z. is on the scientific advisory board of Third Pole, Inc., which has licensed patents on NO generators from MGH. Neither W.M.Z. nor B.Y. holds equity in the company. F.I. declares no conflicts of interest. I.K. is a current employee of Air Liquide, a major provider of home oxygen therapy. A.R.M. receives research funding from Air Liquide, and has consulted for Air Liquide and Third Pole, Inc. No other conflicts of interest exist.

#### References

1. ISAM: Abstracts: International Society for Aerosols in Medicine, 21st Congress, Santa Fe, NM, June 3–7. *J Aerosol Med Pulm Drug Deliv.* 2017;30:A1–A38.
2. Dunne PJ: The clinical impact of new long-term oxygen therapy technology. *Respir Care.* 2009;54:1100–1111.
3. Girardis M, Busani S, Damiani E, Donati A, Rinaldi L, Marudi A, Morelli A, Antonelli M, and Singer M: Effect of conservative vs conventional oxygen therapy on mortality among patients in an intensive care unit: the oxygen-ICU randomized clinical trial. *JAMA.* 2016;316:1583–1589.
4. Gayat E, Imbert N, Roujansky A, Lemasle L, and Fischer M: Influence of fraction of inspired oxygen on noninvasive hemoglobin measurement: parallel assessment of 2 monitors. *Anesth Analg.* 2017;124:1820–1823.
5. Wagstaff TAJ, and Soni N: Performance of six types of oxygen delivery devices at varying respiratory rate. *Anaesthesia.* 2007;62:492–503.
6. Wettstein RB, Shelledy DC, and Peters JI: Delivered oxygen concentrations using low-flow and high-flow nasal cannulas. *Respir Care.* 2005;50:604–609.
7. Casaburi R: Assessing the dose of supplemental oxygen: let us compare methodologies. *Respir Care.* 2005;50:594–595.
8. Bhatraju P, Crawford J, Hall M, and Lang JD, Jr.: Inhaled nitric oxide: current clinical concepts. *Nitric Oxide.* 2015; 50:114–128.
9. Terpolilli NA, Kim S-W, Thal SC, Kataoka H, Zeisig V, Nitzsche B, Klaesner B, Zhu C, Schwarzmaier S, Meissner L, Mamrak U, Engel DC, Drzezga A, Patel RP, Blomgren K, Barthel H, Boltze J, Kuebler WM, and Plesnila N: Inhalation of nitric oxide prevents ischemic brain damage in experimental stroke by selective dilatation of collateral arterioles. *Circ Res.* 2012;110:727–738.
10. Kida K, and Ichinose F: Preventing ischemic brain injury after sudden cardiac arrest using NO inhalation. *Crit Care.* 2014;18:212.
11. Ryter SW, Kim HP, Nakahira K, Zuckerbraun BS, Morse D, and Choi AMK: Protective functions of heme oxygenase-1 and carbon monoxide in the respiratory system. *Antioxid Redox Signal.* 2007;9:2157–2174.
12. Rooney KT, Goldberg HJ, Hunninghake GM, Nakahira K, Siempos II, Flaherty KR, Martinez FJ, Garcia JGN, Lederer DJ, Osorio JC, Raghu G, Villalba JA, Lasky J, Collard HR, Noth I, Machado RF, Steele C, Rosas IO, and Choi AMK: The effect of inhaled low dose carbon monoxide on cytokine/chemokine production in idiopathic pulmonary fibrosis. In: *B110. Novel Therapies and Targets in Fibrosis.* Presented at the American Thoracic Society International Conference Abstracts. American Thoracic Society; 2016: A4542. Available at: [http://www.atsjournals.org/doi/abs/10.1164/ajrccm-conference.2016.193.1\\_MeetingAbstracts.A4542](http://www.atsjournals.org/doi/abs/10.1164/ajrccm-conference.2016.193.1_MeetingAbstracts.A4542) Last viewed on February 5, 2018.
13. Streeter E, Ng HH, and Hart JL: Hydrogen sulfide as a vasculoprotective factor. *Med Gas Res.* 2013;3:9.
14. Jain K, Sethi SK, Damor M, and Jain N: Effects of inhaled nitrous oxide on the induction dose and time requirements of propofol: a prospective, randomized, double-blind study. *Anesth Essays Res.* 2017;11:174–180.
15. Schmitz G, Goode H, Hess L, King K, and Sparkman M (2013). Use of nitrous oxide in the emergency department: a review of the literature. *Emerg Med.* 3:e131. DOI: 10.4172/2165-7548.1000e131
16. Winkler DA, Thornton A, Farjot G, and Katz I: The diverse biological properties of the chemically inert noble gases. *Pharmacol Ther.* 2016;160:44–64.
17. Law LS-C, Lo EA-G, and Gan TJ: Xenon anesthesia: a systematic review and meta-analysis of randomized controlled trials. *Anesth Analg.* 2016;122:678–697.
18. Katz IM, Martin AR, Muller P-A, Terzibachi K, Feng C-H, Caillibotte G, Sandeau J, and Texereau J: The ventilation distribution of helium–oxygen mixtures and the role of inertial losses in the presence of heterogeneous airway obstructions. *J Biomech.* 2011;44:1137–1143.
19. Katz I, Pichelin M, Montesantos S, Majoral C, Martin A, Conway J, Fleming J, Venegas J, Greenblatt E, and Caillibotte G: Using helium-oxygen to improve regional deposition of inhaled particles: mechanical principles. *J Aerosol Med Pulm Drug Deliv.* 2014;27:71–80.
20. Peterson JB, Prisk GK, and Darquenne C: Aerosol deposition in the human lung periphery is increased by reduced-density gas breathing. *J Aerosol Med Pulm Drug Deliv.* 2008;21:159–168.
21. Darquenne C, Fleming JS, Katz I, Martin AR, Schroeter J, Usmani OS, Venegas J, and Schmid O: Bridging the gap between science and clinical efficacy: physiology, imaging,



- and modeling of aerosols in the lung. *J Aerosol Med Pulm Drug Deliv.* 2016;29:107–126.
22. Frostell C, Fratacci MD, Wain JC, Jones R, and Zapol WM: Inhaled nitric oxide. A selective pulmonary vasodilator reversing hypoxic pulmonary vasoconstriction. *Circulation.* 1991;83:2038–2047.
  23. Lundberg JO, Weitzberg E, and Gladwin MT: The nitrate-nitrite-nitric oxide pathway in physiology and therapeutics. *Nat Rev Drug Discov.* 2008;7:156–167.
  24. Gow AJ, and Stamler JS: Reactions between nitric oxide and haemoglobin under physiological conditions. *Nature.* 1998;391:169–173.
  25. Yu B, Bloch KD, and Zapol WM: Hemoglobin based red blood cell substitutes and nitric oxide. *Trends Cardiovasc Med.* 2009;19:103–107.
  26. Kinsella JP, Truog WE, Walsh WF, Goldberg RN, Bancalari E, Mayock DE, Redding GJ, deLemos RA, Sardesai S, McCurnin DC, Moreland SG, Cutter GR, and Abman SH: Randomized, multicenter trial of inhaled nitric oxide and high-frequency oscillatory ventilation in severe, persistent pulmonary hypertension of the newborn. *J Pediatr.* 1997;131(Pt 1):55–62.
  27. Clark RH, Kueser TJ, Walker MW, Southgate WM, Huckaby JL, Perez JA, Roy BJ, Keszler M, and Kinsella JP: Low-dose nitric oxide therapy for persistent pulmonary hypertension of the newborn. *N Engl J Med.* 2000;342:469–474.
  28. Roberts JD, Polaner DM, Zapol WM, and Lang P: Inhaled nitric oxide in persistent pulmonary hypertension of the newborn. *Lancet.* 1992;340:818–819.
  29. Group (NINOS) TNINOS: Inhaled nitric oxide and hypoxic respiratory failure in infants with congenital diaphragmatic hernia. *Pediatrics.* 1997;99:838–845.
  30. Kinsella JP, Neish SR, Shaffer E, and Abman SH: Low-dose inhalation nitric oxide in persistent pulmonary hypertension of the newborn. *Lancet.* 1992;340:819–820.
  31. Committee on Fetus and Newborn: Use of inhaled nitric oxide. *Pediatrics.* 2000;106:344–345.
  32. Ballard RA, Truog WE, Cnaan A, Martin RJ, Ballard PL, Merrill JD, Walsh MC, Durand DJ, Mayock DE, Eichenwald EC, Null DR, Hudak ML, Puri AR, Golombek SG, Courtney SE, Stewart DL, Welty SE, Phibbs RH, Hibbs AM, Luan X, Wadlinger SR, Asselin JM, and Coburn CE: Inhaled nitric oxide in preterm infants undergoing mechanical ventilation. *N Engl J Med.* 2006;355:343–353.
  33. Malhotra R, Hess D, Lewis GD, Bloch KD, Waxman AB, and Semigran MJ: Vasoreactivity to inhaled nitric oxide with oxygen predicts long-term survival in pulmonary arterial hypertension. *Pulm Circ.* 2011;1:250–258.
  34. LW & Wilkins: Late-breaking clinical trial abstracts. *Circulation.* 2015;132:2267–2285.
  35. Subhedar N, and Dewhurst C: Is nitric oxide effective in preterm infants? *Arch Dis Child Fetal Neonatal Ed.* 2007;92:F337–F341.
  36. Lovich MA, Fine DH, Denton RJ, Wakim MG, Wei AE, Maslov MY, Gamero LG, Vasquez GB, Johnson BJ, Roscigno RF, and Gilbert RJ: Generation of purified nitric oxide from liquid N<sub>2</sub>O<sub>4</sub> for the treatment of pulmonary hypertension in hypoxemic swine. *Nitric Oxide Biol Chem.* 2014;37:66–72.
  37. Namihira T, Tsukamoto S, Wang D, Katsuki S, Hackam R, Okamoto K, and Akiyama H: Production of nitric monoxide using pulsed discharges for a medical application. *IEEE Trans Plasma Sci.* 2000;28:109–114.
  38. Namihira T, Katsuki S, Hackam R, Akiyama H, and Okamoto K: Production of nitric oxide using a pulsed arc discharge. *IEEE Trans Plasma Sci.* 2002;30:1993–1998.
  39. Stoffels E, Gonzalvo YA, Whitmore TD, Seymour DL, and Ress JA: A plasma needle generates nitric oxide. *Plasma Sources Sci Technol.* 2006;15:501.
  40. Kühn S, Bibinov N, Gesche R, and Awakowicz P: Non-thermal atmospheric pressure HF plasma source: generation of nitric oxide and ozone for bio-medical applications. *Plasma Sources Sci Technol.* 2009;19:015013.
  41. Massines F, Rabehi A, Decomps P, Gadri RB, Ségur P, and Mayoux C: Experimental and theoretical study of a glow discharge at atmospheric pressure controlled by dielectric barrier. *J Appl Phys.* 1998;83:2950–2957. Available at <http://aip.scitation.org/doi/abs/10.1063/1.367051> (accessed August 17, 2017).
  42. Samaranyake WJM, Miyahara Y, Namihira T, Katsuki S, Hackam R, and Akiyama H: Ozone production by pulsed power in dry air. *IEEE.* 1999;2:1326–1329.
  43. Yu B, Muenster S, Blaesi AH, Bloch DB, and Zapol WM: Producing nitric oxide by pulsed electrical discharge in air for portable inhalation therapy. *Sci Transl Med.* 2015;7:294ra107.
  44. Osamura H, and Abe N: Development of new iridium alloy for spark plug electrodes. SAE International, Warrendale, PA; 1999. <http://papers.sae.org/1999-01-0796> Last viewed on February 5, 2018.
  45. Jehn H, Völker R, and Ismail MI: Iridium losses during oxidation. *Platin Met Rev.* 1978;22:92–97.
  46. Yu B, Blaesi AH, Casey N, Raykhtsaum G, Zazzeron L, Jones R, Morrese A, Dobrynin D, Malhotra R, and Bloch DB: Detection and removal of impurities in nitric oxide generated from air by pulsed electrical discharge. *Nitric Oxide.* 2016;60:16–23.
  47. Berra L, Rodriguez-Lopez J, Rezoagli E, Yu B, Fisher DF, Semigran MJ, Bloch DB, Channick RN, and Zapol WM: Electric plasma-generated nitric oxide: hemodynamic effects in patients with pulmonary hypertension. *Am J Respir Crit Care Med.* 2016;194:1168–1170.
  48. Nocturnal Oxygen Therapy Trial Group: Continuous or nocturnal oxygen therapy in hypoxemic chronic obstructive lung disease: a clinical trial. *Ann Intern Med.* 1980;93:391–398.
  49. Croxton TL, and Bailey WC: Long-term oxygen treatment in chronic obstructive pulmonary disease: recommendations for future research. *Am J Respir Crit Care Med.* 2006;174:373–378.
  50. Office of Information Products and Data Analytics: 2013 CMS statistics: CMS publication 03504. 2013. [www.iso.org/obp/ui/#iso:std:iso:80601:-2-67:ed-1:v1:en](http://www.iso.org/obp/ui/#iso:std:iso:80601:-2-67:ed-1:v1:en) (accessed September 5, 2017).
  51. Ekström M: Clinical usefulness of long-term oxygen therapy in adults. *N Engl J Med.* 2016;375:1683–1684.
  52. Chen JZ, Katz IM, Pichelin M, Zhu K, Caillibotte G, Noga ML, Finlay WH, and Martin AR: Comparison of pulsed versus continuous oxygen delivery using realistic adult nasal airway replicas. *Int J Chron Obstruct Pulmon Dis.* 2017;12:2559–2571.
  53. Byron PR, Hindle M, Lange CF, Longest PW, McRobbie D, Oldham MJ, Olsson B, Thiel CG, Wachtel H, and Finlay WH: In vivo–in vitro correlations: predicting pulmonary drug deposition from pharmaceutical aerosols. *J Aerosol Med Pulm Drug Deliv.* 2010;23(Suppl 2):S59–S69.

54. Grgic B, Finlay WH, Burnell PKP, and Heenan AF: In vitro intersubject and intrasubject deposition measurements in realistic mouth-throat geometries. *J Aerosol Sci.* 2004;35:1025–1040.
55. Golshahi L, Vehring R, Noga ML, and Finlay WH: In vitro deposition of micrometer-sized particles in the extra-thoracic airways of children during tidal oral breathing. *J Aerosol Sci.* 2013;57:14–21.
56. Zhou S, and Chatburn RL: Effect of the anatomic reservoir on low-flow oxygen delivery via nasal cannula: constant flow versus pulse flow with portable oxygen concentrator. *Respir Care.* 2014;59:1199–1209.
57. Martin AR, Katz IM, Lipsitz Y, Terzibachi K, Caillibotte G, and Texereau J: Methods for evaluation of helium/oxygen delivery through non-rebreather facemasks. *Med Gas Res.* 2012;2:31.
58. Rau JL: The inhalation of drugs: advantages and problems. *Respir Care.* 2005;50:367–382.
59. Conway J, Fleming J, Bennett M, and Havelock T: The co-imaging of gamma camera measurements of aerosol deposition and respiratory anatomy. *J Aerosol Med Pulm Drug Deliv.* 2013;26:123–130.
60. Dolovich MB: Measuring total and regional lung deposition using inhaled radiotracers. *J Aerosol Med.* 2001;14(Suppl 1):35–44.
61. Fleming J, Bailey DL, Chan H-K, Conway J, Kuehl PJ, Laube BL, and Newman S: Standardization of techniques for using single-photon emission computed tomography (SPECT) for aerosol deposition assessment of orally inhaled products. *J Aerosol Med Pulm Drug Deliv.* 2012;25(Suppl 1):S29–S51.
62. Fleming JS, Halson P, Conway J, Moore E, Nassim MA, Hashish AH, Bailey AG, Holgate ST, and Martonen TB: Three-dimensional description of pulmonary deposition of inhaled aerosol using data from multimodality imaging. *J Nucl Med.* 1996;37:873–877.
63. Häussermann S, Acerbi D, Brand P, Herpich C, Poli G, Sommerer K, and Meyer T: Lung deposition of formoterol HFA (Atimos®/Forair®) in healthy volunteers, asthmatic and COPD patients. *J Aerosol Med.* 2007;20:331–341.
64. Messian MS, Perry R, Silverberg M, Kaplan AP, and Smaldone GC: Quantitative assays of pharmacologic aerosols used in studying asthma. *J Allergy Clin Immunol.* 1985;76:605–609.
65. Petersson J, Sánchez-Crespo A, Larsson SA, and Mure M: Physiological imaging of the lung: single-photon-emission computed tomography (SPECT). *J Appl Physiol.* 2007;102:468–476.
66. Klocke RA, and Farhi LE: Simple method for determination of perfusion and ventilation-perfusion ratio of the underventilated elements (the slow compartment) of the lung. *J Clin Invest.* 1964;43:2227–2232.
67. Halaweish AF, Moon RE, Foster WM, Soher BJ, McAdams HP, MacFall JR, Ainslie MD, MacIntyre NR, and Charles HC: Perfluoropropane gas as a magnetic resonance lung imaging contrast agent in humans. *Chest.* 2013;144:1300–1310.
68. Fowler WS, Cornish ER, and Kety SS: Lung function studies. VIII. Analysis of alveolar ventilation by pulmonary N<sub>2</sub> clearance curves. *J Clin Invest.* 1952;31:40–50.
69. Becklake MR: A new index of the intrapulmonary mixture of inspired air. *Thorax.* 1952;7:111–116.
70. Verbanck S, and Paiva M: Model simulations of gas mixing and ventilation distribution in the human lung. *J Appl Physiol.* 1990;69:2269–2279.
71. Lewis SM, Evans JW, and Jalowayski AA: Continuous distributions of specific ventilation recovered from inert gas washout. *J Appl Physiol.* 1978;44:416–423.
72. Edelman RR, Hatabu H, Tadamura E, Li W, and Prasad PV: Noninvasive assessment of regional ventilation in the human lung using oxygen-enhanced magnetic resonance imaging. *Nat Med.* 1996;2:1236–1239.
73. Ohno Y, and Hatabu H: Basics concepts and clinical applications of oxygen-enhanced MR imaging. *Eur J Radiol.* 2007;64:320–328.
74. Sá RC, Cronin MV, Henderson AC, Holverda S, Theilmann RJ, Arai TJ, Dubowitz DJ, Hopkins SR, Buxton RB, and Prisk GK: Vertical distribution of specific ventilation in normal supine humans measured by oxygen-enhanced proton MRI. *J Appl Physiol.* 2010;109:1950–1959.
75. Paiva M, and Engel LA: Theoretical studies of gas mixing and ventilation distribution in the lung. *Physiol Rev.* 1987;67:750–796.
76. Sá RC, Asadi AK, Theilmann RJ, Hopkins SR, Prisk GK, and Darquenne C: Validating the distribution of specific ventilation in healthy humans measured using proton MR imaging. *J Appl Physiol.* 2014;116:1048–1056.
77. Tedjasaputra V, Sá RC, Arai TJ, Holverda S, Theilmann RJ, Chen WT, Wagner PD, Davis CK, Prisk GK, and Hopkins SR: The heterogeneity of regional specific ventilation is unchanged following heavy exercise in athletes. *J Appl Physiol.* 2013;115:126–135.
78. Patz MD, Sá RC, Darquenne C, Elliott AR, Asadi AK, Theilmann RJ, Dubowitz DJ, Swenson ER, Prisk GK, and Hopkins SR: Susceptibility to high-altitude pulmonary edema is associated with a more uniform distribution of regional specific ventilation. *J Appl Physiol.* 2017;122:844–852.
79. Sá RC, Zeman KL, Bennett WD, Prisk GK, and Darquenne C: Regional ventilation is the main determinant of alveolar deposition of coarse particles in the supine healthy human lung during tidal breathing. *J Aerosol Med Pulm Drug Deliv.* 2017;30:322–331.
80. Heinonen E, Högman M, and Meriläinen P: Theoretical and experimental comparison of constant inspired concentration and pulsed delivery in NO therapy. *Intensive Care Med.* 2000;26:1116–1123.
81. Martin AR, Jackson C, Katz IM, and Caillibotte G: Variability in uptake efficiency for pulsed versus constant concentration delivery of inhaled nitric oxide. *Med Gas Res.* 2014;4:1.

Received on September 29, 2017  
in final form, November 14, 2017

Reviewed by:  
Sabine Häussermann  
Timothy Corcoran

Address correspondence to:  
Ira Katz, PhD  
Centre de Recherche Paris-Saclay  
1 chemin de la Porte des Loges  
BP 126 Les Loges-en-Josas  
78354 Jouy-en-Josas  
France

E-mail: katzi@lafayette.edu